UCSF
UC San Francisco Previously Published Works

Title

The Causal Role of IL-4 and IL-13 in Schistosoma mansoni Pulmonary Hypertension

Permalink

https://escholarship.org/uc/item/0b26v0n2

Journal

American Journal of Respiratory and Critical Care Medicine, 192(8)

ISSN

1073-449X

Authors

Kumar, Rahul
Mickael, Claudia
Chabon, Jacob
et al.

Publication Date

2015-10-15

DOI

10.1164/rccm.201410-1820oc

Peer reviewed

ORIGINAL ARTICLE

The Causal Role of IL-4 and IL-13 in *Schistosoma mansoni* Pulmonary Hypertension

Rahul Kumar[1], Claudia Mickael[1], Jacob Chabon[1], Liya Gebreab[1], Alleluiah Rutebemberwa[1], Alexandra Rodriguez Garcia[1], Daniel E. Koyanagi[1], Linda Sanders[1], Aneta Gandjeva[1], Mark T. Kearns[2], Lea Barthel[2], William J. Janssen[2], Thais Mauad[3], Angela Bandeira[4], Eric Schmidt[1], Rubin M. Tuder[1], and Brian B. Graham[1]

[1]Program in Translational Lung Research, Department of Medicine, Anschutz Medical Campus, Aurora, Colorado; [2]Department of Medicine, National Jewish Health, Denver, Colorado; [3]Department of Pathology, Sao Paulo University Medical School, Sao Paulo, Brazil; and [4]Department of Medicine, Memorial S. Jose Hospital, Universidade de Pernambuco, Recife, Brazil

Abstract

Rationale: The etiology of schistosomiasis-associated pulmonary arterial hypertension (PAH), a major cause of PAH worldwide, is poorly understood. *Schistosoma mansoni* exposure results in prototypical type-2 inflammation. Furthermore, transforming growth factor (TGF)-β signaling is required for experimental pulmonary hypertension (PH) caused by *Schistosoma* exposure.

Objectives: We hypothesized type-2 inflammation driven by IL-4 and IL-13 is necessary for *Schistosoma*-induced TGF-β–dependent vascular remodeling.

Methods: Wild-type, IL-4$^{-/-}$, IL-13$^{-/-}$, and IL-4$^{-/-}$IL-13$^{-/-}$ mice (C57BL6/J background) were intraperitoneally sensitized and intravenously challenged with *S. mansoni* eggs to induce experimental PH. Right ventricular catheterization was then performed, followed by quantitative analysis of the lung tissue. Lung tissue from patients with schistosomiasis-associated and connective tissue disease–associated PAH was also systematically analyzed.

Measurements and Main Results: Mice with experimental *Schistosoma*-induced PH had evidence of increased IL-4 and IL-13 signaling. IL-4$^{-/-}$IL-13$^{-/-}$ mice, but not single knockout IL-4$^{-/-}$ or IL-13$^{-/-}$ mice, were protected from *Schistosoma*-induced PH, with decreased right ventricular pressures, pulmonary vascular remodeling, and right ventricular hypertrophy. IL-4$^{-/-}$IL-13$^{-/-}$ mice had less pulmonary vascular phospho–signal transducer and activator of transcription 6 (STAT6) and phospho-Smad2/3 activity, potentially caused by decreased TGF-β activation by macrophages. *In vivo* treatment with a STAT6 inhibitor and IL-4$^{-/-}$IL-13$^{-/-}$ bone marrow transplantation also protected against *Schistosoma*-PH. Lung tissue from patients with schistosomiasis-associated and connective tissue disease–associated PAH had evidence of type-2 inflammation.

Conclusions: Combined IL-4 and IL-13 deficiency is required for protection against TGF-β–induced pulmonary vascular disease after *Schistosoma* exposure, and targeted inhibition of this pathway is a potential novel therapeutic approach for patients with schistosomiasis-associated PAH.

Keywords: pulmonary hypertension; schistosomiasis; Th2 cells; transforming growth factor-β

At a Glance Commentary

Scientific Knowledge on the Subject:
Inflammation is likely a key driver in the pathogenesis of many forms of pulmonary arterial hypertension, but specific mechanisms by which inflammation results in vascular disease are unknown. Schistosomiasis is a major cause of pulmonary arterial hypertension worldwide and may be paradigmatic of inflammation driving vascular disease. We and others have previously observed that transforming growth factor-β signaling is required for multiple forms of experimental pulmonary hypertension, including because of chronic hypoxia and Schistosoma exposure.

What This Study Adds to the Field:
We found evidence of type-2 inflammation (IL-4 and IL-13) in mice with experimentally induced pulmonary hypertension via Schistosoma exposure, and deficiency of both IL-4 and IL-13, or treatment with a signal transducer and activator of transcription factor 6 inhibitor, prevented the transforming growth factor-β–induced pulmonary hypertension. We also found evidence of type-2 inflammation in the lungs of patients who died of schistosomiasis-associated pulmonary arterial hypertension and in explanted lung tissue from patients with connective tissue disease–associated pulmonary arterial hypertension.

Schistosomiasis-associated vascular remodeling is a leading cause of pulmonary arterial hypertension (PAH) worldwide, with significant morbidity and mortality (1). Schistosomiasis-associated PAH shares pathologic features with other forms of PAH, such as idiopathic PAH and connective tissue disease (CTD)-associated PAH, including remodeling of vascular media and intima resulting in right ventricular (RV) failure (2). The initial response to Schistosoma is type-1 inflammation induced by worm antigens, marked by production of proinflammatory cytokines including IL-1, IL-12, interferon-γ, and tumor necrosis factor-α in the plasma

and infected tissue (3). Chronic schistosomal infection, like that of other helminths, drives a strong type-2 inflammation, thought to be largely mediated by a CD4$^+$ T helper 2 (Th2) response, while suppressing the type-1 response. This Th2 response, triggered by egg-derived antigens, includes cytokines IL-4, IL-5, IL-10, and IL-13, resulting in fibrosis and granulomas containing lymphocytes, fibrocytes, and macrophages (4).

Among the Schistosoma-triggered type-2 cytokines, IL-4 and IL-13 play critical roles in activation of signaling pathways within cells that regulate cascades of immunologic response (5). Both IL-4 and IL-13 bind heterodimeric receptors including the IL-4Rα subunit, generating common downstream signaling via phosphorylation of signal transducer and activator of transcription factor 6 (STAT6). This signaling may then regulate downstream targets involved in inflammation, fibrosis, and vascular remodeling (6, 7). Mice experimentally exposed to Schistosoma can develop pulmonary hypertension (PH), recapitulating key features of human disease including increased RV pressure, pulmonary vascular remodeling, and RV hypertrophy (8–10). Our recent studies focused on the role of increased intrapulmonary transforming growth factor (TGF)-β1 after Schistosoma exposure: blockade of TGF-β signaling prevented the development of experimental Schistosoma-induced PH (11). In line with the downstream proremodeling effect of TGF-β, its signaling blockade suppressed IL-4 and IL-13 signaling, indicating a positive feedback loop between TGF-β and IL-4/IL-13 in disease propagation (11). However, these studies did not clarify the proximal functional activity of IL-4 and/or IL-13, and how they impact downstream signaling, such as STAT6; moreover, they did not address potential discrete roles of IL-4 and IL-13, identify cells producing or receiving the IL-4 and IL-13 signals, or address mechanisms by which IL-4 and IL-13 lead to TGF-β signaling.

We hypothesized herein that interactions between IL-4, IL-13, and TGF-β signaling are causative of Schistosoma-induced PH, and specifically that IL-4 and/or IL-13 deficiency may protect against TGF-β–induced vascular disease. We found that, unlike schistosomal liver disease (12), Schistosoma-induced PH requires both IL-4

and IL-13, which act proximally and via STAT6 to drive TGF-β signaling and pulmonary vascular remodeling in Schistosoma-induced PH. We also observed evidence of IL-4/IL-13 signaling in pulmonary tissue from individuals who died of schistosomiasis-associated PAH, underscoring the potential clinical relevance. Some of these data have been published in abstracts (13, 14).

Methods

Animals
Wild-type (C57BL6/J) mice were purchased (Taconic, Hudson, NY). IL-4^{GFP} mice (C57BL6/J background) were kindly provided by Dr. Hua Huang (National Jewish Health, Denver, CO) and originally from Dr. William Paul (15). IL-4^{GFP} mice contain GFP in place of the IL-4 transcript; we therefore used IL-4$^{GFP/+}$ mice for flow studies and IL-4$^{GFP/GFP}$ mice as knockout mice in phenotype assessment studies. IL-13^{YFP} mice (Balb/C background) were purchased (Jackson Laboratory, Bar Harbor, ME). IL-13$^{-/-}$ mice (C57BL6/J background) were kindly provided by Dr. Erwin Gelfand (National Jewish Health) (16). IL-4$^{-/-}$IL-13$^{-/-}$ mice (C57BL6/J background) were kindly provided by Dr. Thomas Wynn (National Institute of Allergy and Infectious Diseases/National Institutes of Health). IL-13Rα2$^{-/-}$ mice (C57BL6/J background) were kindly provided by Wyeth/Pfizer (New York, NY). All experimental procedures in rodents were approved by the Animal Care and Use Committee at the University of Colorado Denver. Additional details are provided in the online supplement.

Schistosomiasis Exposure, Bone Marrow Transplantation, and Treatments
Schistosoma mansoni eggs were obtained from infected mice provided by the Biomedical Research Institute. Experimental mice were intraperitoneally sensitized to 240 Schistosoma eggs per gram, and intravenously challenged 2 weeks later with 175 eggs per gram; control mice were unexposed. For bone marrow (BM) transplantation, recipient mice received 10 Gy radiation followed by 1.5×10^6 BM cells, and trimethoprim-sulfadiazine chow for 4 weeks. Mice were treated with the STAT6 pharmacologic inhibitor AS1517499 or vehicle (Axon-Medchem,
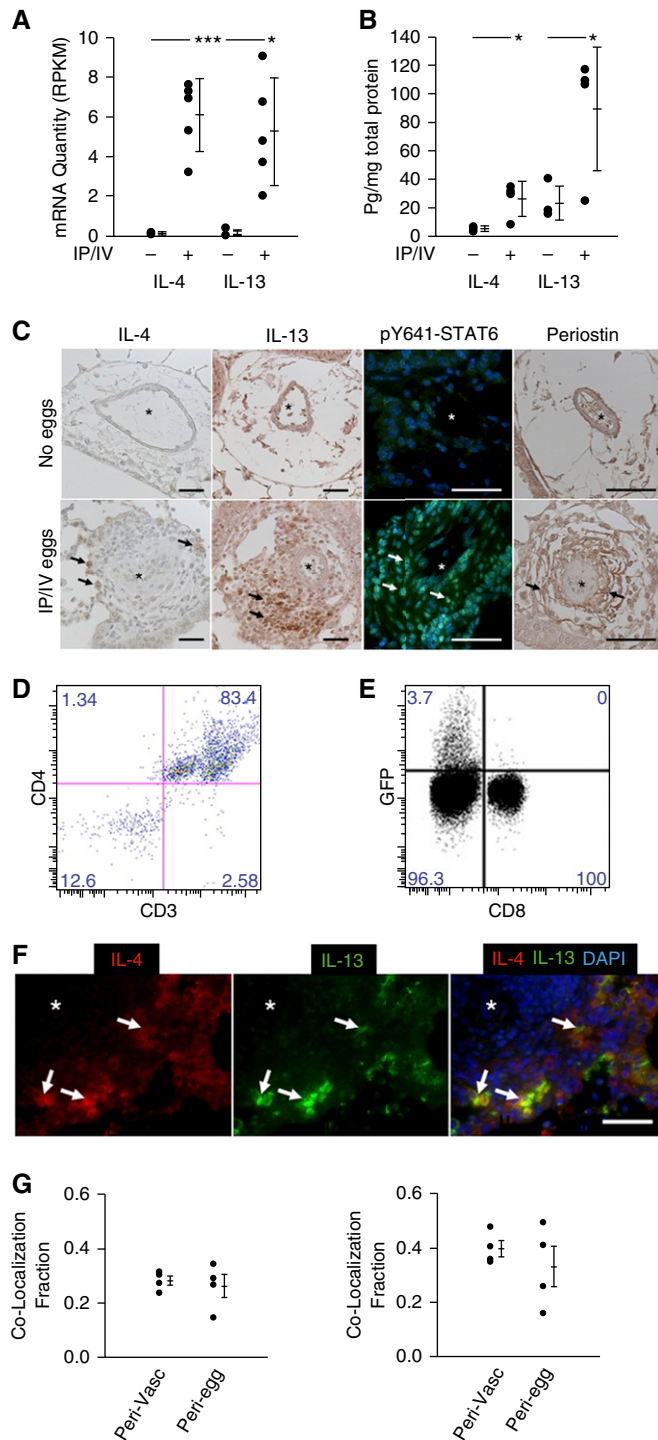
Figure 1. *Schistosoma*-exposed mouse tissue demonstrates evidence of Th2 signaling. (*A*) Whole-lung quantity of IL-4 and IL-13 messenger RNA (mRNA) transcripts (n = 5 samples per group; RPKM; mean ± SD; *t* test, *$P < 0.05$; ***$P < 0.005$). (*B*) IL-4 and IL-13 whole-lung ELISA (mean ± SD; n = 4 samples per group; *t* test, *$P < 0.05$). (*C*) Immunostaining for IL-4, IL-13, phospho–signal transducer and activator of transcription factor 6 (STAT6) and periostin in *Schistosoma*-exposed and unexposed mouse lung tissue (*asterisks*, vessel lumens; *arrows*, representative positive stained cells; *scale bars*, 50 μm). (*D*) Flow cytometry analysis of GFP$^+$ cells from intraperitoneal and intravenous (IP/IV) egg–exposed IL-4^{GFP} mice for CD3$^+$ and CD4$^+$ cells. (*E*) Percentage of CD3$^+$CD4$^+$ and CD3$^+$CD8$^+$ cells in IP/IV egg–exposed mice positive for IL-4^{GFP} (flow studies repeated at least three times). (*F* and *G*) Qualitative (*F*) and quantitative (*G*) colocalization of IL-4 and

Groningen, the Netherlands), and soluble IL-13Rα2 receptor or control peptide (sIL-13Rα2-Fc; Pfizer). Additional details are provided in the online supplement.

PH and Hypertrophy Measurement

Measurement of RV pressure and hypertrophy was performed as previously described using a 1F pressure-volume catheter and measurement of the RV mass (Millar PVR-1035; Millar Instruments, Houston, TX) (8, 11); additional details are provided in the online supplement.

Mouse Protein, RNA, and Flow Cytometry Assessment

Immunostaining was performed on mouse lung tissue, whole-lung lysate protein was quantified by ELISA, and flow cytometry was performed on digested lung tissue using the reagents in Tables E1–E3 in the online supplement. Messenger RNA (mRNA) was quantified using a HiSeq 2000 RNA sequencing (RNA-seq) system (Illumina, San Diego, CA), as previously described; the data are deposited in National Center for Biotechnology Information's GEO dataset GSE49116 (10). Additional details are provided in the online supplement.

Human Tissue Immunostaining

Immunohistochemistry staining was performed on formalin-fixed paraffin-embedded samples using the reagents in Table E4 on three types of lung tissue:

1. *Schistosoma*-PAH: obtained at autopsy from patients who died of schistosomiasis-associated PAH in Brazil.
2. Scleroderma-associated PAH: obtained at the time of explantation by the Pulmonary Hypertension Breakthrough Initiative.
3. Control/failed lung donor: from the Pulmonary Hypertension Breakthrough Initiative.

All human studies were approved by the Colorado Multiple Institutional Review Board and the University of Sao Paulo Ethics Commission.

Image Analysis and Egg Burden Quantification

Mouse lung media and intima thickness was quantified using image processing software (8, 11). Granuloma volumes were estimated using optical rotator stereology (17). *Schistosoma* egg density in mouse lung

tissue was determined using potassium hydroxide digestion (18). Additional details are provided in the online supplement.

Statistical Analysis

Statistical analyses were performed using ProStat (Poly Software, Pearl River, NY). Differences between two groups were assessed with Student's t test and three or more groups with analysis of variance; P less than 0.05 was considered statistically significant.

Results

Evidence of Type-2 Inflammation in Murine Schistosomiasis-Induced Pulmonary Vascular Disease

We have developed a robust and reproducible mouse model of Schistosoma-induced PH using intraperitoneal sensitization followed by intravenous challenge with S. mansoni eggs (8, 10, 11, 19). This model bypasses potentially confounding effects of liver disease and abbreviates the development of PH to 21 days. Overall, the pulmonary pathobiology reproduces several of the key features observed after 4 months following the natural course of infection (8). Whole-lung RNA quantification by RNA-seq revealed significantly higher mRNA transcript quantity of IL-4 and IL-13 in wild-type Schistosoma-exposed mice compared with unexposed mice (Figure 1A). Quantitative analysis of whole-lung IL-4 and IL-13 cytokine levels by ELISA also demonstrated increases with Schistosoma exposure (Figure 1B). Immunostaining similarly revealed an increase in adventitial IL-4, IL-13, phosphorylated STAT6 (phospho-STAT6), and its target periostin in Schistosoma-exposed mice compared with unexposed mice (Figure 1C).

IL-4 and IL-13 Originates in CD4^{+} T Cells

We next sought to identify cellular sources of IL-4 production using flow cytometry to analyze IL-4[GFP] reporter mice, and observed 83.4% of pulmonary GFP^{+} cells were CD3^{+}CD4^{+} T cells, whereas 3.7% of all CD4^{+} T cells were positive for GFP (Figures 1D and 1E). We also used an IL-13[YFP] reporter mouse and observed 1.1% of CD4^{+} T cells were YFP^{+} (see Figure E1).
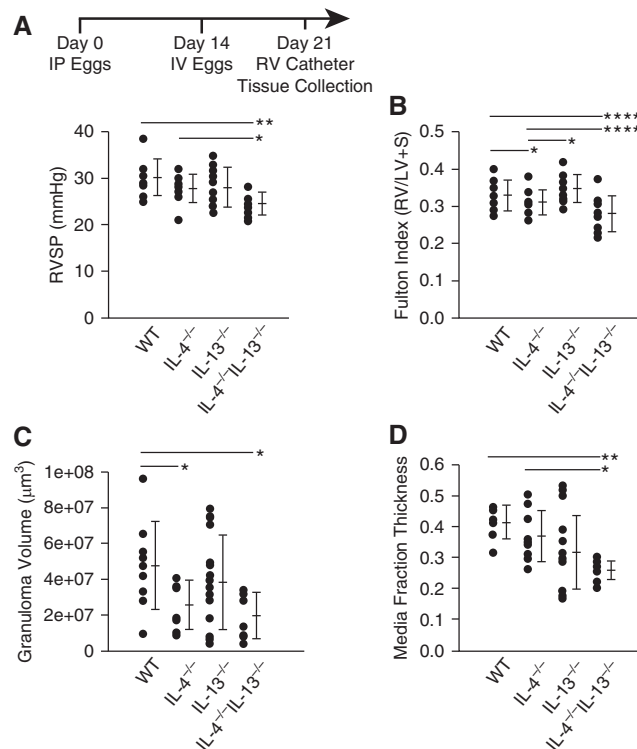

Figure 2. Mice exposed to Schistosoma mansoni eggs develop pulmonary hypertension and vascular remodeling, which is suppressed in the absence of IL-4 and IL-13. (A) Right ventricular systolic pressure (RVSP) of intraperitoneal and intravenous (IP/IV) egg–exposed mice (mean ± SD; n = 9–18 mice per group; analysis of variance (ANOVA), $P = 0.01$; post hoc Tukey test, *$P < 0.05$, **$P < 0.01$). (B) Fulton index (RV/[LV + S]) of IP/IV egg–exposed mice (mean ± SD; n = 9–18 mice per group; ANOVA, $P = 0.001$; post hoc Tukey test, *$P < 0.05$, ****$P < 0.001$). (C) Periegg granuloma volumes in IP/IV egg–exposed mice (mean ± SD; n = 9–18 mice per group; ANOVA, $P = 0.03$; post hoc Tukey test, *$P < 0.05$). (D) Quantitative fractional thickness of the pulmonary vascular media in IP/IV egg exposed mice (mean ± SD; n = 9–18 mice per group; ANOVA $P = 0.007$; post hoc Tukey test, *$P < 0.05$, **$P < 0.01$). LV = left ventricle; RV = right ventricle; S = systolic; WT = wild type.

There was no significant signal for either reporter from CD8^{+} T cells or macrophages (data not shown). Double staining for the IL-4 and IL-13 ligands and quantitative analysis colocalized 30–40% of IL-4 and IL-13 to double-positive cells within both the adventitia and periegg granulomas (Figures 1F and 1G).

IL-4^{−/−}IL-13^{−/−} Mice Exposed to Schistosoma Eggs Have Decreased RV Pressure and Vascular Remodeling

To determine the functional roles of IL-4 and IL-13 in Schistosoma-induced PH, we used singly and doubly deficient IL-4^{−/−} and IL-13^{−/−} mice using our established model of experimental disease. We observed significantly reduced RV systolic pressure (RVSP), RV hypertrophy, and granuloma volumes in Schistosoma-exposed IL-4^{−/−}IL-13^{−/−} mice compared with infected wild-type and single knockout IL-4^{−/−} or IL-13^{−/−} mice (Figures 2A–2C). In Schistosoma-unexposed mice we observed marginal differences in RVSP, RV mass, and vascular thicknesses between these four genotypes (see Figures E2A–E2D). There were no significant differences in left ventricular systolic pressure, right or left ventricular diastolic pressures, heart rate, or body weight between exposed and unexposed mice for all genotypes (see Table E5). Quantitative

---

Figure 1. (Continued). IL-13 using double immunoflorescence analysis (G, left, fraction of IL-4–positive area that colocalizes with IL-13; G, right, fraction of IL-13–positive area that colocalizes with IL-4; asterisk, vessel lumens; arrows, representative double-positive cells; scale bar, 50 μm; plots mean ± SD; n = 4 samples per group; the groups are perivascular/adventitia and periegg/granuloma images). DAPI = 4′,6-diamidino-2-phenylindole; GFP = green fluorescent protein; RPKM = reads per kilobase per million mapped reads.
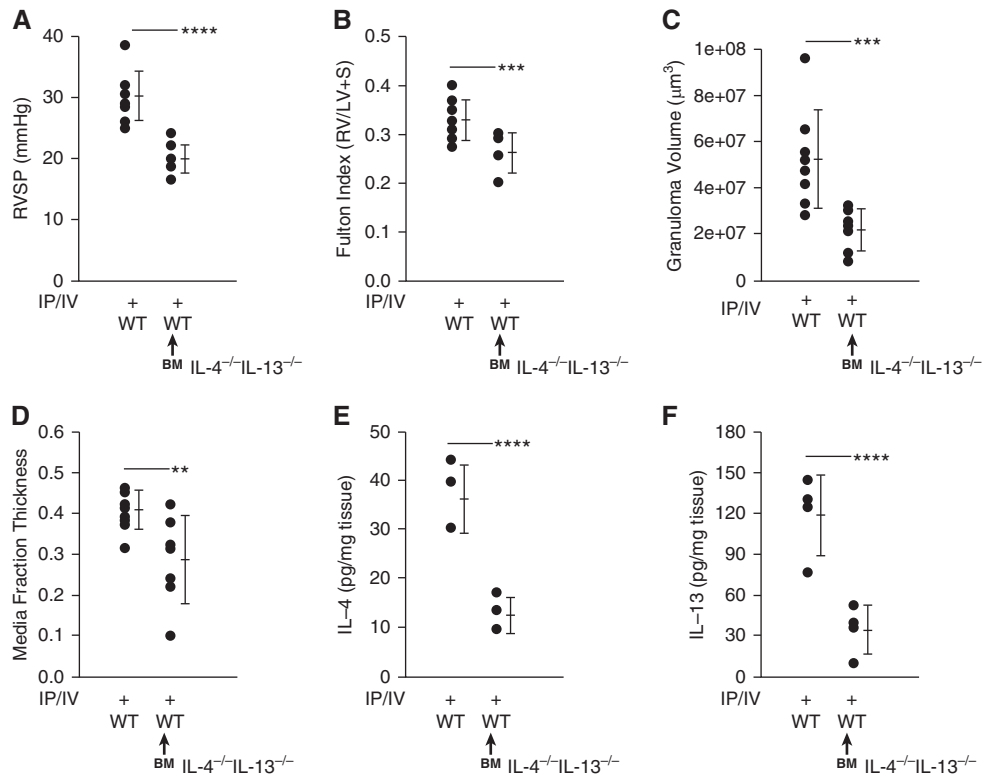
Figure 3. Wild-type (WT) recipients of IL-4$^{-/-}$IL-13$^{-/-}$ bone marrow (BM) showed decreased IL-4 and IL-13 levels and protection against pulmonary hypertension after exposure to *Schistosoma mansoni* eggs. WT and WT recipients of IL-4$^{-/-}$IL-13$^{-/-}$ BM followed by intraperitoneal and intravenous (IP/IV) egg exposure. (*A*) Right ventricular systolic pressure (RVSP) (mean ± SD; n = 8–9 mice per group; *t* test, ****$P < 0.001$). (*B*) Fulton index (RV/[LV + S]) (mean ± SD; n = 8–9 mice per group; *t* test, ***$P < 0.005$). (*C*) Periegg granuloma volume (mean ± SD; n = 8–9 mice per group; *t* test, ***$P < 0.005$). (*D*) Quantitative fractional thickness of the pulmonary vascular media (mean ± SD; n = 8–9 mice per group; *t* test, **$P < 0.01$). (*E*) Concentration of whole-lung IL-4 (mean ± SD; n = 4 mice per group; *t* test, ****$P < 0.001$). (*F*) Concentration of whole-lung IL-13 (mean ± SD; n = 4 mice per group; *t* test, ****$P < 0.001$). LV = left ventricle; RV = right ventricle; S = systolic.

analysis revealed decreased pulmonary artery media thickening in IL-4$^{-/-}$IL-13$^{-/-}$ mice relative to wild-type mice after *Schistosoma* exposure (Figure 2D). We did not observe differences in intima thickness between the different *Schistosoma*-exposed genotypes, concordant with previously observed sparing of intima remodeling in this model in wild-type mice (*see* Figure E2E).

The observed protection in double knockout mice was unlikely related to

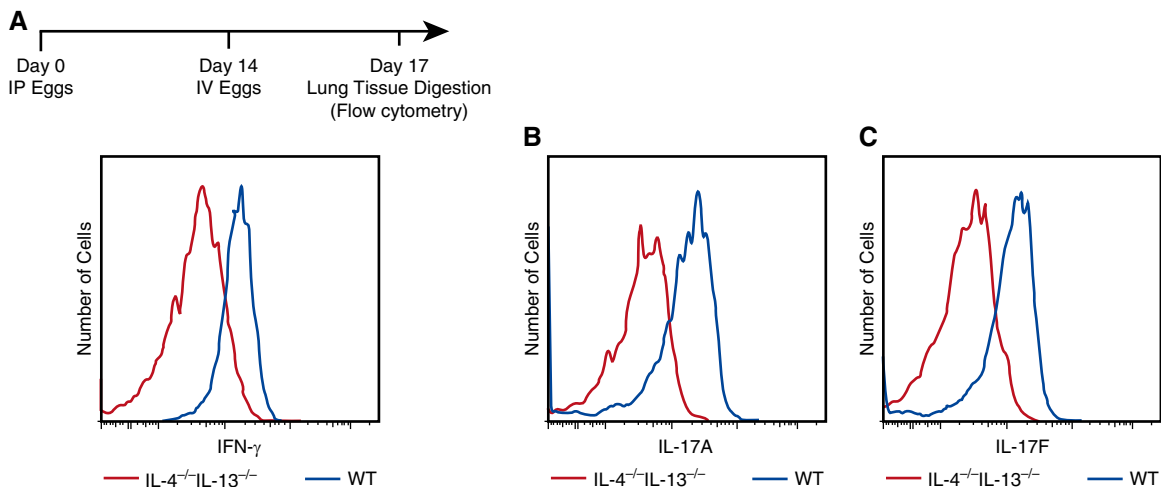**Figure 4.** IL-4$^{-/-}$IL-13$^{-/-}$ mice exposed to *Schistosoma mansoni* eggs have suppressed Th1 and Th17 responses. (*A–C*) Flow cytometric histograms of CD3$^+$CD4$^+$ populations from digested whole-lung tissue, individually gated for IFN-γ (*A*), IL-17A (*B*), and IL-17F (*C*) in intraperitoneal and intravenous (IP/IV) egg–exposed IL-4$^{-/-}$IL-13$^{-/-}$ and wild-type (WT) mice (flow studies repeated at least three times).

inability to clear the parasite, because egg burden 1 week after intravenous challenge did not differ among the four genotypes (*see* Figure E2F). We had previously observed a component of Rho kinase-dependent vasoconstriction in *Schistosoma*-induced PH (11), and now observed increased GTP-bound (active) Rho A in both wild-type and IL-4$^{-/-}$IL-13$^{-/-}$ mice after *Schistosoma* exposure (*see* Figure E3), indicating Rho kinase signaling in this model is IL-4/IL-13 independent.

It was recently reported that IL-13 overexpression can induce PH dependent on the second IL-13 receptor, IL-13Rα2, although it is debated if IL-13Rα2 has functional signaling ability or is a competitive decoy receptor (7, 20–22). We had previously observed that ablation of IL-13Rα2, potentially resulting in IL-13 gain-of-function, enhanced *Schistosoma*-induced PH (8). To address whether this augmented phenotype was IL-13 dependent, we treated IL-13Rα2$^{-/-}$ mice with soluble IL-13Rα2-Fc; indeed, blockade of IL-13 with the soluble receptor chimera prevented the exacerbated *Schistosoma*-PH phenotype (*see* Figures E4A and E4B). We also crossed IL-13Rα2$^{-/-}$ with IL-13$^{-/-}$ mice, and found these mice were also protected from *Schistosoma*-induced PH (*see* Figures E4C and E4D). These data suggest that the augmented PH phenotype observed in *Schistosoma*-exposed IL-13Rα2$^{-/-}$ mice is mediated by IL-13 signaling gain-of-function.

Wild-Type Murine Recipients of IL-4$^{-/-}$IL-13$^{-/-}$ Bone Marrow Are Protected against *Schistosoma*-PH

Having observed a major source of IL-4 and IL-13 to be CD4$^+$ T cells—which are BM derived—we confirmed the compartment responsible for pathogenic IL-4/IL-13 signaling by transferring IL-4$^{-/-}$IL-13$^{-/-}$ BM into irradiated wild-type recipient mice, followed by *Schistosoma* challenge. We found wild-type recipients of IL-4$^{-/-}$IL-13$^{-/-}$ BM were significantly protected from *Schistosoma*-induced PH (Figures 3A–3D). Wild-type mice with IL-4$^{-/-}$IL-13$^{-/-}$ BM also had significantly less whole-lung IL-4 and IL-13 after exposure to *Schistosoma* (Figures 3E and 3F). Of note, BM transplant alone did not have an effect on the phenotype in wild-type recipients of wild-type BM (data not shown).

IL-4$^{-/-}$IL-13$^{-/-}$ Mice Exposed to *Schistosoma* Eggs Do Not Have Compensatory Th1 or Th17 Responses

A possible additive protective mechanism in IL-4$^{-/-}$IL-13$^{-/-}$ mice is compensatory Th1 or Th17 response. To address this question, we analyzed intracellular Th1 and Th17 markers by flow cytometry (e.g., interferon-γ and IL-17A and F, respectively) in CD3$^+$CD4$^+$ cells (Figure 4; *see* Figure E5). *Schistosoma*-exposed IL-4$^{-/-}$IL-13$^{-/-}$ mice showed in fact suppressed Th1 and Th17 responses compared with wild-type mice, whereas individual IL-4$^{-/-}$
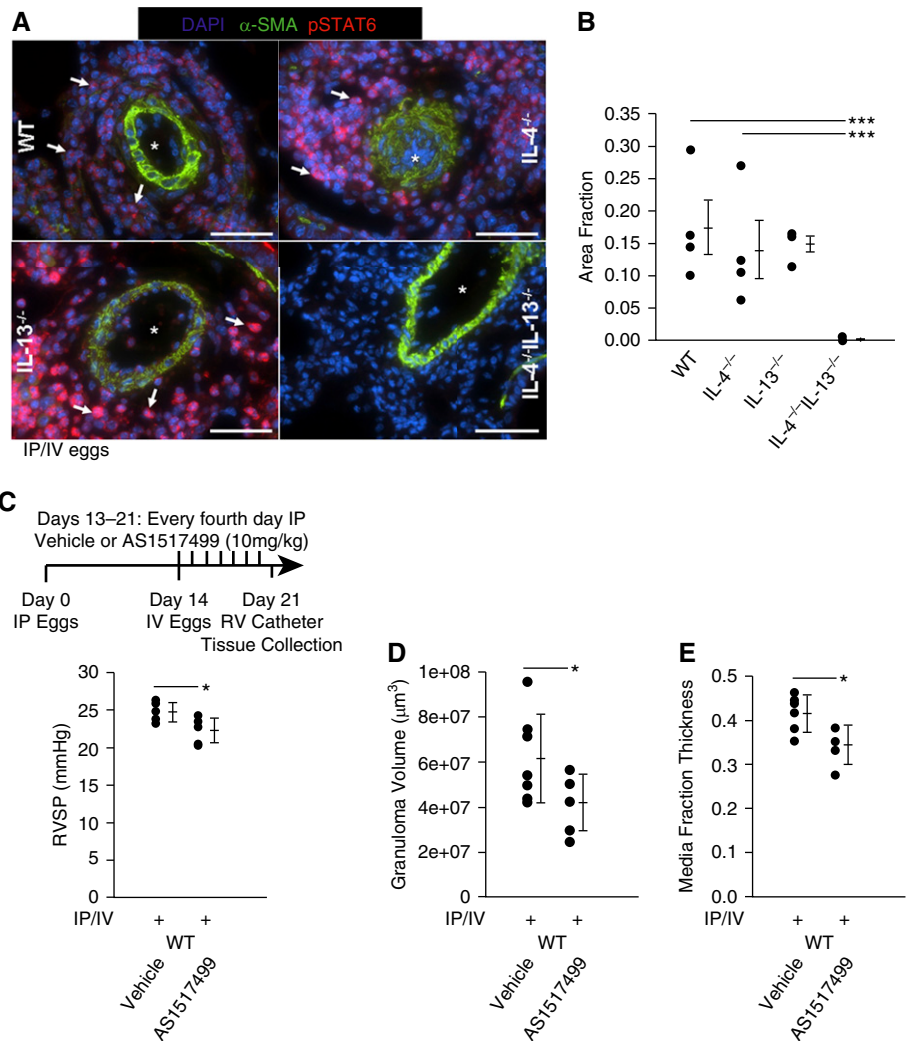
Figure 5. *Schistosoma*-exposed IL-4$^{-/-}$IL-13$^{-/-}$ mice have decreased phospho–signal transducer and activator of transcription factor 6 (STAT6), and STAT6 inhibition prevents *Schistosoma*-pulmonary hypertension. (*A*) Representative images showing representative immunostaining for phospho-Y641-STAT6 in *Schistosoma*-exposed wild-type (WT), IL-4$^{-/-}$, IL-13$^{-/-}$, and IL-4$^{-/-}$IL-13$^{-/-}$ mice (images representative of n = 4/group; *asterisks*, vessel lumens; *arrows*, representative positive stained cells; *scale bars*, 50 μm). (*B*) Quantification of area staining positive for phospho-STAT6 in the pulmonary vascular adventitia in *Schistosoma*-exposed WT, IL-4$^{-/-}$, IL-13$^{-/-}$, and IL-4$^{-/-}$IL-13$^{-/-}$ mice (mean ± SD; n = 4 specimens per group; analysis of variance, P = 0.009; *post hoc* Tukey test, ***P < 0.005). (*C–E*) IP/IV egg–exposed WT mice treated with the STAT6 inhibitor AS1517499 or equivalent volume of vehicle: right ventricular systolic pressure (RVSP) (mean ± SD; n = 7 mice per group; *t* test *P < 0.05) (*C*); granuloma volume (mean ± SD; n = 7 mice per group; *t* test *P < 0.05) (*D*); and quantitative fractional thickness of the pulmonary vascular media (mean ± SD; n = 7 mice per group; *t* test *P < 0.05) (*E*). α-SMA = α-smooth muscle actin; DAPI = 4′,6-diamidino-2-phenylindole; IP/IV = intraperitoneal and intravenous; RV = right ventricle.

and IL13$^{-/-}$ did not have a change in Th1 or Th17 responses compared with wild-type (*see* Figures E5C and E5D).

A potential mechanism for persistent PH in singly-deficient IL-4$^{-/-}$ or IL-13$^{-/-}$ mice is compensatory up-regulation of the partner cytokine. However, after *Schistosoma* exposure, compared with wild-type mice, the concentration of IL-4 in IL-13$^{-/-}$ mice was partially suppressed ($P < 0.05$), and the concentration of IL-13 in IL-4$^{-/-}$ mice was significantly suppressed ($P < 0.01$) (*see* Figure E6), suggesting a positive rather than a negative feedback loop between the two Th2 cytokines, consistent with other reports (23, 24).

IL-4$^{-/-}$IL-13$^{-/-}$ Mice Exposed to *Schistosoma* Have Abrogated Phosphorylated STAT6 Signaling

IL-4 and IL-13 regulate gene expression through shared receptors that trigger phosphorylation of STAT6. Phospho-STAT6 immunostaining revealed no significant signal in unexposed wild-type, IL-4$^{-/-}$, IL-13$^{-/-}$, and IL-4$^{-/-}$IL-13$^{-/-}$ mice (*see* Figure E7). In *Schistosoma*-exposed mice, phospho-STAT6 signal was observed in the adventitia in wild-type and individual IL-4$^{-/-}$ or IL-13$^{-/-}$ mice, but was completely abrogated in IL-4$^{-/-}$IL-13$^{-/-}$ mice (Figures 5A and 5B). There was no significant media or intima signal for phospho-STAT6 in wild-type or IL-4$^{-/-}$IL-13$^{-/-}$ mice (*see* Figure E8).

We had previously observed increased phospho-STAT3 (a target of IL-6 signaling) in *Schistosoma*-exposed mice and *Schistosoma*-associated PAH lung tissue (10). We additionally observed phospho-STAT1 immunostaining in *Schistosoma*-exposed mice (*see* Figure E9A). We now found decreased phospho-STAT3, but no change in phospho-STAT1, in IL-4$^{-/-}$IL-13$^{-/-}$ *Schistosoma*-exposed mice compared with wild-type mice (*see* Figures E9 and E10, respectively).

Blockade of STAT6 Signaling Protects against *Schistosoma*-PH

Considering a potential therapeutic translation of our findings to human disease, we tested the pharmacologic STAT6 inhibitor AS1517499 in *Schistosoma*-exposed wild-type mice (25). AS1517499, as compared with vehicle alone, resulted in significant reduction of *Schistosoma*-PH by RVSP, granuloma size, and media thickness

(but not RV hypertrophy) (Figures 5C–5E; *see* Figure E11A). There was no difference in IL-4 or IL-13 levels after AS1517499 treatment (*see* Figures E11B and E11C), confirming that STAT6 is downstream of IL-4/IL-13 signaling, as expected.

IL-4$^{-/-}$IL-13$^{-/-}$ Mice Exposed to *Schistosoma* Have Suppressed TGF-β Signaling

Increased TGF-β family signaling has been implicated in multiple forms of human and experimental PH. Importantly, enhanced TGF-β signaling is present in patients with schistosomiasis-associated PAH and *Schistosoma*-exposed mice (11). Earlier, we observed that wild-type but not IL-4$^{-/-}$IL-13$^{-/-}$ mice have a two-fold increase in TGF-β1 mRNA quantity in whole-lung lysates, and *Schistosoma*-exposed wild-type mice have increased expression of the canonical TGF-β target phospho-Smad2/3 in the pulmonary intima, media, and adventitia (11). Now we performed
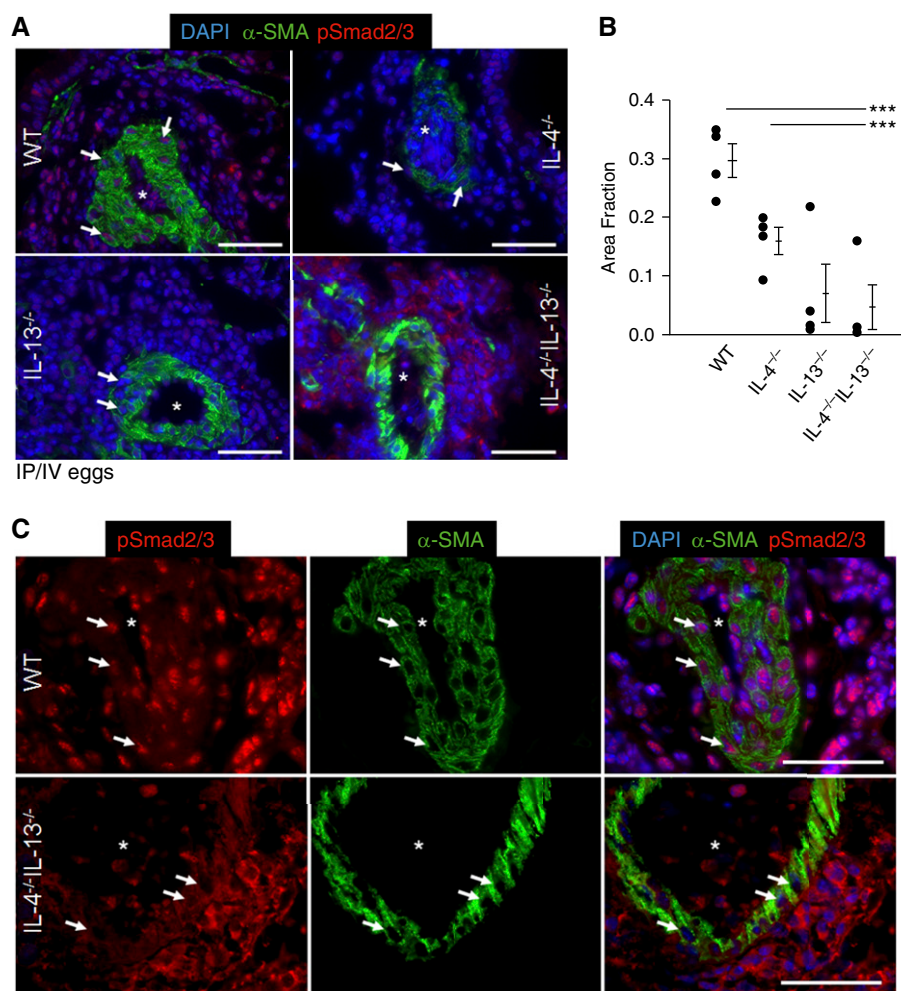
IP/IV eggs

Figure 6. Nuclear phospho-Smad2/3 in the media is decreased in IL-4$^{-/-}$IL-13$^{-/-}$ *Schistosoma*-exposed mice. (*A*) Representative images showing immunostaining for phospho-Smad2/3 and α-smooth muscle actin (α-SMA) in *Schistosoma*-exposed wild-type (WT), IL-4$^{-/-}$, IL-13$^{-/-}$, and IL-4$^{-/-}$IL-13$^{-/-}$ mice (images representative of n = 4/group; *asterisks*, vessel lumens; *arrows*, representative positive nuclear-stained cells; *scale bars*, 50 μm). (*B*) Quantification of the fraction of DAPI-positive pixels that also stain positive for phospho-Smad2/3 in the media of *Schistosoma*-exposed WT, IL-4$^{-/-}$, IL-13$^{-/-}$, and IL-4$^{-/-}$IL-13$^{-/-}$ mice (mean ± SD; n = 4 specimens per group; analysis of variance, $P = 0.002$; *post hoc* Tukey test, ***$P < 0.005$). (*C*) Higher-magnification (×60 oil lens) representative images showing immunostaining for phospho-Smad2/3 and α-smooth muscle actin in *Schistosoma*-exposed WT and IL-4$^{-/-}$IL-13$^{-/-}$ mice (*asterisks*, vessel lumens; *arrows*, representative media cells; *scale bars*, 50 μm). DAPI = 4′,6-diamidino-2-phenylindole; IP/IV = intraperitoneal and intravenous.

a detailed analysis of phospho-Smad2/3 expression in IL-4 and IL-13 deficiency, revealing the increased phospho-Smad2/3 expression in *Schistosoma*-exposed wild-type mice was minimally suppressed in IL-4$^{-/-}$ and IL-13$^{-/-}$ mice (Figure 6A). However, the pulmonary vasculature of *Schistosoma*-exposed IL-4$^{-/-}$IL-13$^{-/-}$ mice showed phospho-Smad2/3 expression, but this was predominantly detected in the cytoplasm, rather than the nucleus, where it needs to translocate to act as a transcription factor for TGF-β–dependent genes (Figures 6B and 6C). Nuclear phospho-Smad2/3 was also partially decreased in wild-type mice treated with AS1517499 (*see* Figure E12). There was no significant vascular phospho-Smad2/3 in unexposed mice (*see* Figure E13). Moreover, we observed that, in this model, phosphorylated Smad1/5/8 (a BMPR2 signaling target) was not affected

by either *Schistosoma* exposure or IL-4/IL-13 deficiency (*see* Figure E14).

We also immunostained for TGF-β1 ligand in infected wild-type, individual, and double IL-4$^{-/-}$IL-13$^{-/-}$ mice using an antibody that detects both active and latent TGF-β1 (with minimal cross-reactivity to TGF-β2/3) (Figures 7A–7D). We costained for macrophages, because these adventitial cells potentially represent a key source for TGF-β1 production and/or activation after exposure to *Schistosoma*. Although the area of TGF-β1 staining was similar in all genotypes of mice exposed to *Schistosoma* (Figures 7A and 7B), there was absence of macrophages and TGF-β1-macrophage colocalization in IL-4$^{-/-}$IL-13$^{-/-}$ mice compared with wild-type and singly deficient mice (Figures 7A, 7C, and 7D). Coupled with data indicating suppressed downstream signaling via phospho-Smad2/3

in IL-4$^{-/-}$IL-13$^{-/-}$ mice (Figure 6), this observation suggests a key function of Th2-stimulated macrophages may be TGF-β1 activation rather than synthesis (*see* Figure E15). There was no significant TGF-β1 ligand present in uninfected mice (*see* Figure E16).

Evidence of Type-2 Inflammation in Human Schistosomiasis-associated Pulmonary Vascular Disease

To seek further support for the relevance of our observations to clinical disease, we analyzed markers of type-2 inflammation in the lungs of patients with *Schistosoma*-associated PAH, CTD-associated PAH, and normal control subjects. Only paraffin-embedded tissue was available for this analysis. Immunostaining and semiquantitative analysis revealed increased presence of IL-13, IL-4Rα,
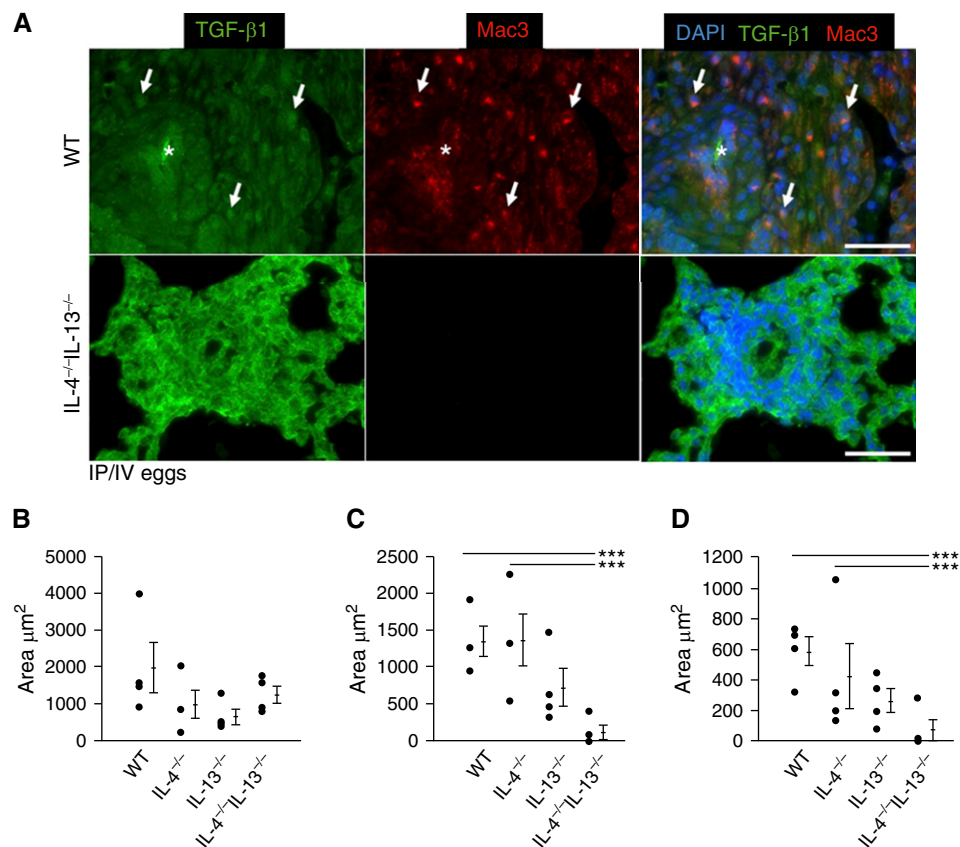

Figure 7. Macrophage density and transforming growth factor (TGF)-β1–macrophage colocalization is decreased in IL-4$^{-/-}$IL-13$^{-/-}$ *Schistosoma*-exposed mice. (*A*) Representative images showing double immunofluorescence staining for TGF-β ligand and Mac3 (macrophage marker; images representative of n = 4/group; *asterisks*, vessel lumens; *arrows*, representative positive double-stained cells; *scale bars*, 50 μm). (*B–D*) Quantitative analysis of area in the adventitia that stains positive for TGF-β1 (mean ± SD; n = 4 specimens per group; analysis of variance [ANOVA], *P* = NS) (*B*), Mac3 (macrophages; mean ± SD; n = 4 specimens per group; ANOVA, *P* = 0.011; *post hoc* Tukey test, ***P* < 0.005) (*C*), and colocalization of both TGF-β1 and macrophages (mean ± SD; n = 4 specimen per group; ANOVA, *P* = 0.011; *post hoc* Tukey test, ***P* < 0.005) (*D*) in *Schistosoma*-exposed wild-type, IL-4$^{-/-}$, IL-13$^{-/-}$, and IL-4$^{-/-}$IL-13$^{-/-}$ mice. DAPI = 4′,6-diamidino-2-phenylindole; IP/IV = intraperitoneal and intravenous; NS = not significant; WT = wild-type.

phospho-STAT6, and periostin in the pulmonary vasculature of patients with CTD-associated PAH and *Schistosoma*-PAH compared with normal control subjects (Figure 8; *see* Table E6). Periostin in particular was primarily located in a subendothelial compartment (*see* Figures E17 and E18). Quantitative analysis of periostin immunostaining revealed increased vascular stain intensity in *Schistosoma*-PAH compared with control samples (*see* Figure E19). We also analyzed IL-13Rα1, IL-13Rα2, IL-4, and RELM-β (the equivalent of murine RELM-α), and observed no significant differences between diseased and control samples (data not shown).

Discussion

Our findings reveal a key pathogenic role for the Th2 immune response–mediated cytokines IL-4 and IL-13 in *Schistosoma*-associated PH. We previously reported increased TGF-β1 mRNA induced by *Schistosoma* exposure was absent in IL-4$^{-/-}$IL-13$^{-/-}$ mice, and that blockade of TGF-β1 at the level of the ligand,

receptor, or intracellular signaling molecule Smad3 protected against *Schistosoma*-PH. Building on these prior observations, we now identified the TGF-β signaling and PH induced by *Schistosoma* results from nonredundant IL-4 and IL-13 signaling, largely originating from CD4$^+$ T cells, and mediated by STAT6 signaling in adventitial cells, potentially macrophages in particular. Identification of type-2 inflammation in human PAH lung tissue supports the clinical relevance and potential therapeutic implications of our findings.

The combined requirement of IL-4 and IL-13 to induce *Schistosoma*-PH may result from summative or synergistic effects. Summative signaling via STAT6 to exceed a threshold for Th2 inflammation-driven PH is suggested by the reported sufficiency of IL-13 overexpression alone to induce PH (20). However, we also observed a feedback system among IL-4, IL-13, and TGF-β suggestive of an amplifying, synergistic effect. Among potential downstream signaling pathways, we observed decreased phospho-STAT3 signal in IL-4/IL-13 double-deficient mice, indicating STAT3 is downstream of Th2 signaling in this model. In other contexts, Th1 and Th17 signaling

may increase when Th2 inflammation is suppressed (26, 27), but in this model we did not find a compensatory Th1 or Th17 increase in IL-4$^{-/-}$IL-13$^{-/-}$ mice.

We observed that a major source of IL-4 and IL-13 is CD4$^+$ T cells; the BM-derived origin of pathologic IL-4/IL-13 was confirmed by protection in wild-type recipients of IL-4$^{-/-}$IL-13$^{-/-}$ BM. *In vitro*, IL-4 is the major driver of the Th2 phenotype (24), but in this model we found that blockade of both IL-4 and IL-13 was required for suppression of *Schistosoma*-PH. Our data are in line with the report that IL-4 deficiency resulted in partial suppression of *Schistosoma* granulomas, whereas additive IL-13 blockade using soluble IL-13Rα2-Fc near-completely abrogated the granulomas (28).

Potentially key intermediate cells receiving IL-4/IL-13 signals and then activating TGF-β signaling are interstitial macrophages. IL-4 and IL-13 are known activators of "alternative" (also called M2 phenotype) macrophages, which may be potential sources of TGF-β (29). In this study, we observed *Schistosoma*-exposed IL-4$^{-/-}$IL-13$^{-/-}$ mice had fewer perivascular macrophages and concurrently less nuclear phospho-Smad2/3 signal in the vascular media, but persistent total TGF-β1 (by immunostaining). A key role of IL-4/IL-13 may thus be activation of TGF-β1 via phospho-STAT6 signaling. The precise mechanism by which STAT6 signaling leads to TGF-β1 activation is not yet elucidated, but it has been reported that IL-13 overexpression can activate TGF-β1 via increased matrix metalloproteinase-9 (30), and TGF-β1 signaling can be modulated by concurrent STAT6 binding to gene promoters (31).

The clinical significance of our rodent model is supported by the expression of key type-2 inflammation molecules in diseased human tissue. Our analysis of *Schistosoma*-PAH tissue is limited to immunohistochemistry: excessive autofluoresence in these samples makes quantification analysis by immunofluorescence challenging. We have also previously been unsuccessful at reliable mRNA quantification from this tissue, but anticipate performing more detailed and quantitative analyses in the future. The presence of type-2 inflammation in human lung tissue is corroborated by a recent study reporting increased TGF-β1 and a trend toward increased IL-13 concentrations in
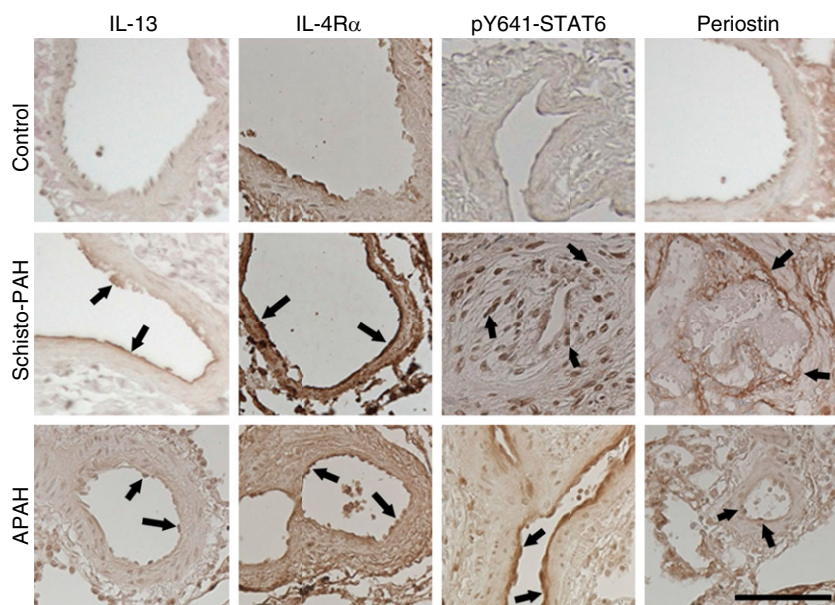
Figure 8. Human lung tissue immunostaining demonstrates increased Th2 signaling. Immunostaining for the type 2 signaling molecules IL-13, IL-4Rα, phospho–signal transducer and activator of transcription factor 6 (STAT6), and periostin in lung tissue of patients with *Schistosoma*–pulmonary arterial hypertension (Schisto-PAH) and connective tissue disease–associated PAH (APAH) compared with normal control subjects. Semiquantitative analysis is reported in Table E6. The images are representative of n = 5–11/group; *arrows* indicate representative positive vascular staining; *scale bar*, 100 μm.

the serum of patients with *Schistosoma*-PAH compared with those with *Schistosoma*-liver disease but without PAH (32). Serum periostin concentration has also been shown to correlate with dermatologic disease in patients with scleroderma, although not interstitial lung disease (33).

Having observed that preclinical blockade of STAT6 using a pharmacologic inhibitor resulted in prevention of the experimental PH phenotype (although did not modulate RVH, possibly because of dosage or differential effects on the pulmonary vasculature vs. RV tissue), novel therapeutic approaches in *Schistosoma*-PAH (and potentially other forms resulting from type-2 inflammation) may thus include targeting both IL-4 and IL-13

cytokines, inhibiting STAT6, and/or blocking TGF-β signaling in the vasculature. Of note, *Schistosoma*-PAH patients would need to be first treated with antihelmenthic therapy before such biologic inhibitors, to eradicate any active infection, because antiinflammatory therapy suppresses the host-parasite response. Such an approach is warranted, however, because modern series report patients are dying of this disease despite antihelminthic treatment and in the absence of active infection (19, 34).

In summary, we observed combined deficiency of IL-4 and IL-13 is required to protect against TGF-β–mediated vascular disease caused by *Schistosoma* exposure. Our study underscores potential molecular targets in *Schistosoma*-

induced and other inflammatory forms of human PH. ■

References

1. Hovnanian A, Hoette S, Fernandes CJ, Jardim C, Souza R. Schistosomiasis associated pulmonary hypertension. *Int J Clin Pract Suppl* 2010;(165):25–28.
2. Simonneau G, Gatzoulis MA, Adatia I, Celermajer D, Denton C, Ghofrani A, Gomez Sanchez MA, Krishna Kumar R, Landzberg M, Machado RF, *et al.* Updated clinical classification of pulmonary hypertension. *J Am Coll Cardiol* 2013; 62(25 Suppl):D34–D41.
3. Boros DL, Whitfield JR. Enhanced Th1 and dampened Th2 responses synergize to inhibit acute granulomatous and fibrotic responses in murine *schistosomiasis mansoni*. *Infect Immun* 1999;67:1187–1193.
4. Burke ML, Jones MK, Gobert GN, Li YS, Ellis MK, McManus DP. Immunopathogenesis of human schistosomiasis. *Parasite Immunol* 2009;31:163–176.
5. Jiang H, Harris MB, Rothman P. IL-4/IL-13 signaling beyond JAK/STAT. *J Allergy Clin Immunol* 2000;105:1063–1070.
6. Hershey GK. IL-13 receptors and signaling pathways: an evolving web. *J Allergy Clin Immunol* 2003;111:677–690, quiz 691.
7. Fichtner-Feigl S, Strober W, Kawakami K, Puri RK, Kitani A. IL-13 signaling through the IL-13alpha2 receptor is involved in induction of TGF-beta1 production and fibrosis. *Nat Med* 2006;12:99–106.
8. Graham BB, Mentink-Kane MM, El-Haddad H, Purnell S, Zhang L, Zaiman A, Redente EF, Riches DW, Hassoun PM, Bandeira A, *et al.* Schistosomiasis-induced experimental pulmonary hypertension: role of interleukin-13 signaling. *Am J Pathol* 2010;177:1549–1561.
9. Crosby A, Jones FM, Southwood M, Stewart S, Schermuly R, Butrous G, Dunne DW, Morrell NW. Pulmonary vascular remodeling correlates with lung eggs and cytokines in murine schistosomiasis. *Am J Respir Crit Care Med* 2010;181:279–288.
10. Graham BB, Chabon J, Kumar R, Kolosionek E, Gebreab L, Debella E, Edwards M, Diener K, Shade T, Bifeng G, *et al.* Protective role of IL-6 in vascular remodeling in *Schistosoma* pulmonary hypertension. *Am J Respir Cell Mol Biol* 2013;49:951–959.
11. Graham BB, Chabon J, Gebreab L, Poole J, Debella E, Davis L, Tanaka T, Sanders L, Dropcho N, Bandeira A, *et al.* Transforming growth factor-β signaling promotes pulmonary hypertension caused by *Schistosoma mansoni*. *Circulation* 2013;128:1354–1364.
12. Kaviratne M, Hesse M, Leusink M, Cheever AW, Davies SJ, McKerrow JH, Wakefield LM, Letterio JJ, Wynn TA. IL-13 activates a mechanism of tissue fibrosis that is completely TGF-beta independent. *J Immunol* 2004;173:4020–4029.
13. Kumar R, Chabon J, Gebreab L, Garcia AR, Koyanangi D, Sanders L, Tuder R, Graham B. IL-4 and IL-13 are necessary for pulmonary hypertension induced by *Schistosoma mansoni* [abstract]. *Am J Respir Crit Care Med* 2014;189:A4145.
14. Kumar R, Chabon J, Gebreab L, Garcia AR, Koyanangi D, Sanders L, Tuder R, Graham B. Role of IL-4 and IL-13 in *Schistosoma*-induced pulmonary hypertension [abstract]. *FASEB J* 2014;28:LB780.
15. Hu-Li J, Pannetier C, Guo L, Löhning M, Gu H, Watson C, Assenmacher M, Radbruch A, Paul WE. Regulation of expression of IL-4 alleles: analysis using a chimeric GFP/IL-4 gene. *Immunity* 2001;14:1–11.
16. Park JW, Taube C, Yang ES, Joetham A, Balhorn A, Takeda K, Miyahara N, Dakhama A, Donaldson DD, Gelfand EW. Respiratory syncytial virus-induced airway hyperresponsiveness is independent of IL-13 compared with that induced by allergen. *J Allergy Clin Immunol* 2003;112:1078–1087.
17. Tandrup T, Gundersen HJ, Jensen EB. The optical rotator. *J Microsc* 1997;186:108–120.
18. Cheever AW. Conditions affecting the accuracy of potassium hydroxide digestion techniques for counting *Schistosoma mansoni* eggs in tissues. *Bull World Health Organ* 1968;39:328–331.
19. Graham BB, Chabon J, Bandeira A, Espinheira L, Butrous G, Tuder RM. Significant intrapulmonary *Schistosoma* egg antigens are not present in schistosomiasis-associated pulmonary hypertension. *Pulm Circ* 2011;1:456–461.
20. Cho WK, Lee CM, Kang MJ, Huang Y, Giordano FJ, Lee PJ, Trow TK, Homer RJ, Sessa WC, Elias JA, *et al.* IL-13 receptor α2-arginase 2 pathway mediates IL-13-induced pulmonary hypertension. *Am J Physiol Lung Cell Mol Physiol* 2013;304:L112–L124.
21. Morimoto M, Zhao A, Sun R, Stiltz J, Madden KB, Mentink-Kane M, Ramalingam T, Wynn TA, Urban JF Jr, Shea-Donohue T. IL-13 receptor alpha2 regulates the immune and functional response to *Nippostrongylus brasiliensis* infection. *J Immunol* 2009;183:1934–1939.
22. Chiaramonte MG, Mentink-Kane M, Jacobson BA, Cheever AW, Whitters MJ, Goad ME, Wong A, Collins M, Donaldson DD, Grusby MJ, *et al.* Regulation and function of the interleukin 13 receptor alpha 2 during a T helper cell type 2-dominant immune response. *J Exp Med* 2003;197:687–701.
23. Olsan EE, Mukherjee S, Wulkersdorfer B, Shillingford JM, Giovannone AJ, Todorov G, Song X, Pei Y, Weimbs T. Signal transducer and activator of transcription-6 (STAT6) inhibition suppresses renal cyst growth in polycystic kidney disease. *Proc Natl Acad Sci USA* 2011;108:18067–18072.
24. Zhu J, Paul WE. Peripheral CD4+ T-cell differentiation regulated by networks of cytokines and transcription factors. *Immunol Rev* 2010;238:247–262.
25. Chiba Y, Todoroki M, Nishida Y, Tanabe M, Misawa M. A novel STAT6 inhibitor AS1517499 ameliorates antigen-induced bronchial hypercontractility in mice. *Am J Respir Cell Mol Biol* 2009;41:516–524.

26. Hoffmann KF, Cheever AW, Wynn TA. IL-10 and the dangers of immune polarization: excessive type 1 and type 2 cytokine responses induce distinct forms of lethal immunopathology in murine schistosomiasis. *J Immunol* 2000;164:6406–6416.

27. He R, Kim HY, Yoon J, Oyoshi MK, MacGinnitie A, Goya S, Freyschmidt EJ, Bryce P, McKenzie AN, Umetsu DT, *et al*. Exaggerated IL-17 response to epicutaneous sensitization mediates airway inflammation in the absence of IL-4 and IL-13. *J Allergy Clin Immunol* 2009;124:761–70.e1.

28. Chiaramonte MG, Schopf LR, Neben TY, Cheever AW, Donaldson DD, Wynn TA. IL-13 is a key regulatory cytokine for Th2 cell-mediated pulmonary granuloma formation and IgE responses induced by *Schistosoma mansoni* eggs. *J Immunol* 1999;162:920–930.

29. Duffield JS. The inflammatory macrophage: a story of Jekyll and Hyde. *Clin Sci (Lond)* 2003;104:27–38.

30. Lee CG, Homer RJ, Zhu Z, Lanone S, Wang X, Koteliansky V, Shipley JM, Gotwals P, Noble P, Chen Q, *et al*. Interleukin-13 induces tissue fibrosis by selectively stimulating and activating transforming growth factor beta(1). *J Exp Med* 2001;194:809–821.

31. Takaki H, Ichiyama K, Koga K, Chinen T, Takaesu G, Sugiyama Y, Kato S, Yoshimura A, Kobayashi T. STAT6 Inhibits TGF-beta1-mediated Foxp3 induction through direct binding to the Foxp3 promoter, which is reverted by retinoic acid receptor. *J Biol Chem* 2008;283:14955–14962.

32. Ferreira RdeC, Montenegro SM, Domingues AL, Bandeira AP, Silveira CA, Leite LA, Pereira CdeA, Fernandes IM, Mertens AB, Almeida MO. TGF beta and IL13 in *Schistosomiasis mansoni* associated pulmonary arterial hypertension; a descriptive study with comparative groups. *BMC Infect Dis* 2014;14:282.

33. Yamaguchi Y, Ono J, Masuoka M, Ohta S, Izuhara K, Ikezawa Z, Aihara M, Takahashi K. Serum periostin levels are correlated with progressive skin sclerosis in patients with systemic sclerosis. *Br J Dermatol* 2013;168:717–725.

34. Fernandes CJ, Dias BA, Jardim CV, Hovnanian A, Hoette S, Morinaga LK, Souza S, Suesada M, Breda AP, Souza R. The role of target therapies in schistosomiasis-associated pulmonary arterial hypertension. *Chest* 2012;141:923–928.